Individual and temporal variation in pathogen load predicts long-term impacts of an emerging infectious disease

Konstans Wells[1,2,6], Rodrigo K. Hamede[3], Menna E. Jones[3], Paul A. Hohenlohe[4], Andrew Storfer[5], Hamish I. McCallum[2]

1 Department of Biosciences, Swansea University, Singleton Campus, Wallace Building, Swansea SA2 8PP, UK.

2 Environmental Futures Research Institute, Griffith University, Brisbane QLD 4111, Australia.

3 School of Biological Sciences, University of Tasmania, Hobart, Tasmania 7001, Australia.

4 Institute for Bioinformatics and Evolutionary Studies, Department of Biological Sciences, University of Idaho, Moscow, ID 83844, USA.

5 School of Biological Sciences, Washington State University, Pullman, WA 99164-4236 USA.

6 E-mail: k.l.wells@swansea.ac.uk

Running head: Tasmanian devil facial tumour disease

ABSTRACT

Emerging infectious diseases increasingly threaten wildlife populations. Most studies focus on managing short-term epidemic properties, such as controlling early outbreaks. Predicting long-term endemic characteristics with limited retrospective data is more challenging. We used individual-based modelling informed by individual variation in pathogen load and transmissibility to predict long-term impacts of a lethal, transmissible cancer on Tasmanian devil (*Sarcophilus harrisii*) populations. For this, we employed Approximate Bayesian Computation to identify model scenarios that best matched known epidemiological and demographic system properties derived from ten years of data after disease emergence, enabling us to forecast future system dynamics. We show that the dramatic devil population declines observed thus far are likely attributable to transient dynamics (initial dynamics after disease emergence). Only 21% of matching scenarios led to devil extinction within 100 years following devil facial tumour disease (DFTD) introduction, whereas DFTD faded out in 57% of simulations. In the remaining 22% of simulations, disease and host coexisted for at least 100 years, usually with long-period oscillations. Our findings show that pathogen extirpation or host-pathogen coexistence are much more likely than the DFTD-induced devil extinction, with crucial management ramifications. Accounting for individual-level disease progression and the long-term outcome of devil-DFTD interactions at the population-level, our findings suggest that immediate management interventions are unlikely to be necessary to ensure the persistence of Tasmanian devil populations. This is because strong population declines of devils after disease emergence do not necessarily translate into long-term population declines at equilibria. Our modelling approach is widely applicable to other host-pathogen systems to predict disease impact beyond transient dynamics.

KEYWORDS

disease burden; long-periodicity oscillation; population viability; Tasmanian devil; transmissible cancer; wildlife health

INTRODUCTION

Emerging infectious diseases most often attract attention because their initial impacts on host populations are frequently severe (de Castro and Bolker 2005, Smith et al. 2009). Following the initial epidemic and transient dynamic behaviour, long-term outcomes include pathogen fadeout, host extinction, or long-term endemicity with varying impacts on the host population size (Hastings 2004, Benton et al. 2006, Cazelles and Hales 2006). Predicting which of these long-term outcomes may occur on the basis of initial transient dynamics is very challenging and conclusions about possible disease effects on population viability based on early epidemic dynamics can be misleading with regard to long-term dynamics. For example, disease spread in a newly exposed population may slow down after reduction of the pool of susceptible individuals and coevolutionary processes between a pathogens virulence and host defence mechanism may further impact long-term dynamics.

Nevertheless, predicting the long-term consequences of an infectious disease as early as possible in the emergence process is important for management. If the disease has a high likelihood of ultimately leading to host extinction, then strategies such as stamping out infection by removing all potentially infectious individuals may be justifiable, despite short-term impacts on the host species and ethical considerations (McCallum and Hocking 2005). Resource-intensive strategies such as establishing captive breeding populations protected from disease or translocating individuals to locations separated from infected populations may also be justified (McCallum and Jones 2006). In contrast, if impacts are transitory, then a

preferred strategy may be to avoid interference to allow a new long-term endemic disease state or pathogen extinction to be reached as quickly as possible (Gandon et al. 2013). Longer-term evolutionary processes can operate to ultimately reduce the impact of the disease on the host population (Fenner 1983, Kerr 2012), and inappropriate disease management strategies may slow down evolution of both host and pathogen.

Models of infectious diseases in the early stages of emergence typically focus on estimating R_0, the number of secondarily infected individuals when one infected individual is introduced into a wholly susceptible population (Lloyd-Smith et al. 2005). This is a key parameter for devising strategies to limit invasion or control an outbreak because it allows the estimation of vaccination or removal rates necessary to eradicate disease. However, by definition, it does not include density dependent factors and is therefore sometimes insufficient to predict the long-term consequences of disease introduction into a new population (Heesterbeek 2002).

Most existing models for infectious disease are based around compartmental Susceptible – Exposed – Infected – Recovered epidemiological models (S-E-I-R), which rely on a strict assumption of homogeneity of individuals within compartments (Anderson and May 1991). There is a parallel literature for macroparasitic infections, which assumes both a stationary distribution of parasites amongst hosts and that parasite burden is determined by the number of infective stages the host has encountered (Anderson and May 1978). For many pathogens, pathogen load on (or inside) an individual typically changes following infection as a result of within-host processes, causing temporal shifts in transmission and host mortality rates. For example, the volume of transmissible tumours on Tasmanian devils (*Sarcophilus harrisii*) increases through time, with measurable impacts on survival (Wells et al. 2017) and likely temporal increases in transmission probability to uninfected devils that bite into the growing tumour mass (Hamede et al. 2013). Similarly, increasing burden of the amphibian

chytrid fungus *Batrachochytrium dendrobatidis* on individual frogs after infection limits host survival, with important consequences for disease spread and population dynamics (Briggs et al. 2010, Wilber et al. 2016). Burdens of the causative agent of white nose syndrome, *Pseudogymnoascus destructans*, which threatens numerous bat species in North America, similarly increase on most individuals during the period of hibernation (Langwig et al. 2015). The additional time dependence introduced by within-host pathogen growth can have a major influence on the dynamics of host-pathogen interactions as uncovered by nested models that link within- and between-host processes of disease dynamics (Gilchrist and Coombs 2006, Mideo et al. 2008). Such dynamics are poorly captured by conventional compartmental and macroparasite model structures. Thus, connecting across the scales of within- and between-host dynamics remains a key challenge in understanding infectious disease epidemiology (Gog et al. 2015).

Here we develop an individual-based model to explore the long-term impact of devil facial tumour disease (DFTD), a transmissible cancer, on Tasmanian devil populations. DFTD is a recently emerged infectious disease, first detected in 1996 in north-eastern Tasmania (Hawkins et al. 2006). It is caused by a clonal cancerous cell line, which is transmitted by direct transfer of live tumour cells when devils bite each other (Pearse and Swift 2006, Jones et al. 2008, Hamede et al. 2013). DFTD is nearly always fatal and largely affects individuals that are otherwise the fittest in the population (Wells et al. 2017). Population declines to very low numbers concomitant with the frequency-dependent transmission of DFTD led to predictions of devil extinctions, based on compartmental epidemiological models (McCallum et al. 2009, Hamede et al. 2012).

Fortunately, the local devil extinctions predicted from these early models have not occurred (McCallum et al. 2009). There is increasing evidence that rapid evolutionary changes have taken place in infected devil populations, particularly in loci associated with

disease resistance and immune response (Epstein et al. 2016, Pye et al. 2016, Wright et al. 2017). Moreover, we recently reported that the force of infection (the rate at which susceptible individuals become infected) increases over a time period of as long as six years (~3 generations) after initial local disease emergence and that the time until death after initial infection may be as long as two years (Wells et al. 2017). Therefore, despite high lethality, the rate of epidemic increase appears to be relatively slow, prompting predictive modelling of population level impacts over time spans well beyond those covered by field observations.

In general, there are three potential long-term outcomes of host-pathogen interactions: host extinction, pathogen extirpation, and host-pathogen coexistence. To determine the likelihood of each of these outcomes in a local population of Tasmanian devils, we used individual-based simulation modelling (Fig. 1) and pattern matching, based on ten years of existing field data, to project population trajectories for Tasmanian devil populations over 100 years following DFTD introduction.

MATERIALS AND METHODS

Model framework

We implemented a stochastic individual-based simulation model of coupled Tasmanian devil (*Sarcophilus harrisii*) demography and devil facial tumour disease (DFDT) epidemiology. A full model description with overview of design, concept, and details (Grimm et al. 2006) can be found in Appendix S1. In brief, we aimed to simulate the impact of DFTD on Tasmanian devil populations and validate 10^6 model scenarios of different random input parameters (26 model parameters assumed to be unknown and difficult or impossible to estimate from empirical studies, see Appendix S1: Table S1) by matching known system level properties (disease prevalence and population structure, see Appendix S1: Fig. S2) derived from a wild population studied over ten years after the emergence of DFTD (Hamede et al. 2015). In

particular, running model scenarios for 100 years prior to, and after the introduction of DFTD, we explored the extent to which DFTD causes devil populations to decline or become extinct. Moreover, we aimed to explore whether input parameters such as the latency period of DFTD or the frequencies of disease transmission between individuals of different ages can be identified by matching simulation scenarios to field patterns of devil demography and disease prevalence.

Entities in the model are individuals that move in weekly time steps (movement distance θ) within their home ranges and may potentially engage in disease-transmitting biting behaviour with other individuals (Fig 1). Birth-death processes and DFTD epidemiology are modelled as probabilities according to specified input parameter values for each scenario. In each time step, processes are scheduled in the following order: 1) reproduction of mature individuals (if the week matches the reproductive season), 2) recruitment of juveniles into the population, 3) natural death (independent of DFTD), 4) physical interaction and potential disease transmission, 5) growth of tumours, 6) DFTD-induced death, 7) movement of individuals, 8) aging of individuals.

The force of infection $\lambda_{i,t}$, i.e. the probability that a susceptible individual *i* acquires DFTD at time *t* is given as the sum of the probabilities of DFTD being transmitted from any interacting infected individual *k* (with $k \in 1 \ldots K$, with *K* being the number of all individuals in the population excluding *i*):

$$\lambda_{i,t} = \left[\sum_{k \in K} \beta_{A(i)} \beta_{A(k)} \left(\frac{N_t}{C}\right)^{\delta} \left(\frac{1}{1+(1-r_{i,t})\omega}\right) \left(\frac{1}{1+(1-r_{k,t})\omega}\right) \left(\frac{V_{k,t}}{V_{max}}\right)^{\gamma}\right] I_{\eta}$$

Here, the disease transmission coefficient is composed of the two factors $\beta_{A(i)}$ and $\beta_{A(k)}$, each of which accounts for the age-specific interaction and disease transmission rate for individuals *i* and *k* according to their age classes *A*. N_t is the population size at time *t* and *C* is the carrying capacity of the study region; the scaling factor δ accounts for possible increase in

interactions frequency with increasing population size if $\delta > 0$. The parameter $r_{i,t}$ is a Boolean indicator of whether an individual recently reproduced and ω is a scaling factor that determines the difference in $\lambda_{i,t}$ resulting from interactions of reproductively active and non-reproducing individuals. $V_{k,t}$ is the tumour load of individual k, V_{max} is the maximum tumour load, and γ is a scaling factor of how $\lambda_{i,t}$ changes with tumour load of infected individuals. The parameter I_η is a Boolean indicator of whether two individuals are located in a spatial distance < η that allows interaction and disease transmission (i.e. only individuals in distances < η can infect each other). We considered individuals as 'reproductively active' ($r_{i,t}$=1) for eight weeks after a reproduction event.

DFTD-induced mortality Ω_{size} (modelled as odds ratios in relation to demographic mortality rates with values between 0 and 1) accounts for tumour size, while tumour growth was modelled as a logistic function with the growth parameter α sampled as an input parameter. We allowed for latency periods τ between infection and the onset of tumour growth, which was also sampled as an input parameter. We assumed no recovery from DFTD, which appears be very rare in the field (Pye et al. 2016).

Notably, sampled scaling factor values of zero for δ, ω, and γ correspond to model scenarios with homogeneous interaction frequencies and disease transmission rates independent of population size, reproductive status and tumour load, respectively, while values of η = 21 km assume that individuals can infect each other independent of spatial proximity (i.e. individuals across the entire study area can infect each other). The sampled parameter space included scenarios that omitted *i)* effects of tumour load on infection and survival propensity, *ii)* effect of spatial proximity on the force of infection between pairs of individuals and *iii)* both effects of tumour load and spatial proximity, in each of 1,000 scenarios. This sampling design was used to explicitly assess the importance of modelling individual tumour load and space use for accurately representing the system dynamics.

Model validation and summary

To resolve the most realistic model structures and assumptions from a wide range of possibilities and to compare simulation output with summary statistics from our case study (a devil population at West Pencil Pine in western Tasmania) (Wells et al. 2017), we used likelihood-free Approximate Bayesian Computation (ABC) for approximating the most likely input parameter values, based on the distances between observed and simulated summary statistics (Toni et al. 2009). We used the '*neuralnet*' regression method in the R package *abc* (Csillery et al. 2012). Prediction error was minimized by determining the most accurate tolerance rate and corresponding number of scenarios considered as posterior (distribution of parameter values from scenarios selected to best match empirical evidence according to ABC) through a subsampling cross validation procedure as implemented in the *abc* package. For this, leave-one-out cross validation was used to evaluate the out-of-sample accuracy of parameter estimates (using a subset of 100 randomly selected simulated scenarios), with a prediction error estimated for each input parameter (Csillery et al. 2012); this step facilitates selecting the most accurate number of scenarios as a posterior sample. However, we are aware that none of the scenarios selected as posterior samples entirely represents the true system dynamics. We identified $n = 122$ scenarios (tolerance rate of 0.009, Appendix S1: Fig. S2) as a reasonable posterior selection with minimized prediction error but sufficiently large sample size to express uncertainty in estimates. The distribution of summary statistics was tested against the summary statistics from our case study as a goodness of fit test, using the '*gfit*' function in the *abc* package (with a p-value of 0.37 indicating reasonable fit, Appendix S1: Fig. S3, S4).

We generated key summary statistics from the case study, in which DFTD was expected to have been introduced shortly before the onset of the study (Hamede et al. 2015),

and a pre-selection of simulation scenarios, in which juveniles never comprised > 50% of the population, DFTD prevalence at end of 10-year-period was between 10 and 70%, and the age of individuals with growing tumours was ≥ 52 weeks. Hereafter, we refer to 'prevalence' as the proportion of free-ranging devils (individuals ≥ 35 weeks old) with tumours of sizes ≥ 0.1 cm^3; we do so to derive a measure of prevalence from simulations that is comparable to those inferred from the 10 years of field data. Summary statistics were: 1) mean DFTD prevalence over the course of 10 years, 2) mean DFTD prevalence in the 10^{th} year only, 3) autocorrelation value for prevalence values lagged over one time step (capturing short-term changes in DFTD prevalence), 4) three coefficient estimates of a cubic regression model of the smoothed ordered difference in DFTD prevalence (fitting 3^{rd} order orthogonal polynomials of time for smoothed prevalence values using the loess function in R with degree of smoothing set to $\alpha = 0.75$ in order to capture the overall temporal changes in DFTD prevalence), 5) phase in seasonal population fluctuations, calculated from sinusoidal model fitted to the number of trappable individuals in different time steps (capturing population fluctuations due to seasonal birth pulses), 6) regression coefficient of a linear model of the changing proportions of individuals ≥ 3years old in the trappable population over the course of 10 years (accounting for the known shift in demographic structure; DFTD dispatches mostly mature and reproductively active devils). Summary statistics for the simulations were based on the 37 selected weekly time steps after the introduction of DFTD that matched the time sequences of capture sessions in the case study, which included records in ca. three months intervals (using the first 30 time steps only for population sizes, as the empirical estimates from the last year of field data may be subject to data censoring bias). Overall, these summary statistics aimed to describe general patterns rather than reproducing the exact course of population and disease prevalence changes over time, given that real systems would not repeat themselves for any given dynamics (Wood 2010). Additionally, unknown factors

not considered in the model may contribute to the observed temporal changes in devil abundance and disease prevalence.

As results from our simulations, we considered the posterior distributions of the selected input parameters (as adjusted parameter values according to the ABC approach utilised) and calculated the frequency and timing of population or disease extirpation from the 100 years of simulation after DFTD introduction of the selected scenarios. All simulations and statistics were performed in R version 3.4.3 (R Development Core Team 2017). We used wavelet analysis based on Morlet power spectra as implemented in the R package *WaveletComp* (Roesch and Schmidbauer 2014) to identify possible periodicity at different frequencies in the time series of population sizes (based on all free-ranging individuals) for scenarios in which DFTD persisted at least 100 years.

For estimating the sensitivity of the three possible long-term outcomes (devil extirpation, DFTD extirpation, coexistence) to variation in the posterior estimates of key parameters (i.e. the likely parameter values obtained through the ABC approach), we used boosted regression trees using the '*gbm.step'* routine (binomial error structure, learning rate of 0.001, tree complexity of 5, k-fold cross-validation procedure) in the R package *dismo* (Elith et al. 2008). Similar approaches to global sensitivity analysis were recently applied to eco-epidemiological models (Wells et al. 2015, Drawert et al. 2017).

RESULTS

For scenarios that best matched empirical mark-recapture data, 21% of posterior scenarios (26 out of 122) led to devil population extirpation in timespans of 13 – 42 years (mean = 21, SD = 8; ~7-21 generations) after introduction of DFTD (Fig. 2). In contrast, the disease was lost in 57% of these posterior scenarios (69 out of 122), with disease extirpation taking place 11 – 100 years (mean = 29, SD = 22) post-introduction (Fig. 2). Loss of DFTD from local

populations therefore appears to be much more likely than devil population extirpation, given no other factor than DFTD reducing devil vital rates. Moreover, fluctuations in host and pathogen after the introduction of DFTD exhibited long-period oscillations in most cases (Fig. 3). In the 27 selected scenarios in which DFTD persisted in populations for 100 years after disease introduction, population size 80-100 years after disease introduction was smaller and more variable (mean = 137, SD = 36) than population sizes prior to the introduction of DFTD (mean = 285, SD = 3; Fig. 4). The average DFTD prevalence 80-100 years after disease introduction remained < 40% (mean = 14%, SD = 4%; Fig. 4). Most wavelet power spectra of these scenarios showed long-period oscillations over time periods between 261 – 1040 weeks (corresponding to 5 – 20 years) (Appendix S1: Fig. S5).

Inference of input parameters was only possible for some parameters, whereas 95% credible intervals for most of the posterior distributions were not distinguishable from the (uniformly) sampled priors. Notably, the posterior mode for the latency period (τ) was estimated as 50.5 weeks (95% credible interval 48.5 – 52.6 weeks, for unadjusted parameters values the 95% was 22.9 – 94.3 weeks), providing a first estimate of this latent parameter from field data (Appendix S1: Fig. S6, Table S2). The posterior of the DFTD-induced mortality factor (odds relative to un-diseased devils) for tumours < 50 cm^3 ($\Omega_{<50}$) was constrained to relatively large values (Appendix S1: Fig. S6), supporting empirical estimates that small tumours are unlikely to cause significant mortality of devils. Posterior distributions of weekly movement distances (θ) and the spatial distance over which disease-transmitting interactions took place (η), in turn, allowed no clear estimates of these parameters (Appendix S1: Fig. S6). Notably, the 122 scenarios selected as posteriors all explicitly accounted for the effect of tumour load on infection and survival, while 90% of selected scenarios included spatial proximity of individuals as influencing disease transmission (i.e. selected scenarios comprised 110 models that included both the effect of tumour load and spatial proximity,

while 12 models included tumour load but not spatial proximity). Sensitivity analysis revealed that the long-term outcomes of extinctions (DFTD or devils) versus coexistence were dependent on a suite of parameters related to spatial aspects of transmission, density dependence on transmission and disease progression on individual devils (Appendix S1: Fig. S7, Fig. S8).

DISCUSSION

Our results suggest that DFTD will not necessarily cause local Tasmanian devil extinction or even long-term major declines, whereas the extirpation of DFTD or coexistence/endemicity is much more likely. In cases where DFTD persists in local devil populations in the long-term, oscillations with relatively long periods (5-20 years, corresponding to 2-10 generations) appear likely. These predictions are starkly different from those derived from previous compartmental models, which considered all devils with detectable tumours to be equally infectious and assumed exponentially distributed time delays. These models predicted extinction (McCallum et al. 2009), as did models with more realistic gamma distributed time delays or with delay-differential equations that incorporated field-derived parameter estimates of transmission and mortality rates (Beeton and McCallum 2011). These previous models, however, differ also from our approach in that they ignore spatial structure and do not account for the uncertainty in unknown parameters such as disease-induced mortality and disease transmission rates.

The predictions from our individually-based model, derived from 10 years of observational data at our case study site (West Pencil Pine), are consistent with observations now emerging from long-term field studies of the dynamics of Tasmanian devils and DFTD (Lazenby et al. 2018). No Tasmanian devil population has yet become extinct – and populations persist, albeit in low numbers, where disease has been present the longest (e.g., at

wukalina/Mount William National Park and at Freycinet, where DFTD emerged, respectively, at least 21 and 17 years ago) (Epstein et al. 2016). Also, a considerable decline in DFTD prevalence has been observed in recent years at Freycinet (Sebastien Comte, unpublished data). These study sites did not contribute to the fitting of our model and at least to some extent constitute an independent validation and test of the model predictions. Our modelling results suggest that observed population dynamics of devils and DFTD do not require evolutionary changes, although there is evidence of rapid evolution in disease-burdened devil populations (Epstein et al. 2016) similar to rapid evolution in other vertebrates when subjected to intense selection pressure (Christie et al. 2016, Campbell-Staton et al. 2017).

One of the differences between earlier models and those we present here is the inclusion of tumour growth, with mortality and transmission rates that depend on individual disease burden. Inclusion of burden-dependent dynamics results in additional and qualitatively different time delays than those incorporated in previous models. Tumours take time to grow before they have a major impact on host survival and become highly infectious (Hamede et al. 2017, Wells et al. 2017). This slows the spread of DFTD and its impact on devil population fluctuations. It also means that parameters estimated from field data, without taking tumour growth into account, may not adequately represent the system dynamics (McCallum et al. 2009).

McCallum et al. (2009) and Beeton & McCallum (2011) used an informal rejection method to conclude that the observed dynamics were inconsistent with density-dependent transmission, because, in an SEI (susceptible-exposed-infected) model framework, the observed high prevalence coupled with population decline could only be derived assuming frequency-dependent transmission. This led to predictions of devil extinction. In contrast, our model, which includes spatial aspects of the dynamics in addition to tumour growth, suggests

that there is some density-dependence in transmission, as the posterior distribution for the parameter describing density dependence δ has a mode close to 1 (Appendix S1: Fig. S6). This density dependence may be important in contributing to the increased likelihood of devil population persistence predicted by our model.

Our models suggest that documented dramatic population declines during the first 10 years or so of the DFTD epizootic may represent just the first peak of a classical epidemic (Bailey 1975). Long-term predictions from our models suggest, however, that DFTD is a slow burning disease with population changes governed by long-term oscillations.

It is well known, both from simple Lotka-Volterra models and from a range of empirical studies, that consumer–resource interactions have a propensity to cycle, driven by the time delays inherent in these systems (Murdoch et al. 2003). Disease burden-dependent demographic and epidemiological parameters, together with burden growth within the host, add additional time delays, both lengthening any oscillations and increasing the likelihood that they will be maintained in the longer term. Apparently, such time-delays increase the probability of host-pathogen coexistence, similar to predator-prey dynamics, rather than host or pathogen extirpation. Grounded in theory and a reasonable body of modelling studies of other wildlife diseases, disease-induced population extinction appears to be more generally an exception rather than the rule, unless host populations are very small, or unless there are reservoir species that are tolerant of infection (de Castro and Bolker 2005). Although we found DFTD extirpation 11-100 years after its emergence to be more likely than devil-DFTD coexistence, we believe that recognising the slow burning spread of DFTD and possible long-term oscillations is of practical importance. If both DFTD extirpation and coexistence need to be considered on decadal time spans, immediate management actions after disease emergence and initial population declines are not necessarily essential, if the goal is to maintain presence of devils, even with lower population densities in the case of coexistence (Fig. 4).

375

376 The approach we apply here – coupling the flexibility of individual-based models to account
377 for heterogeneity in disease burden and space use with Approximate Bayesian Computation
378 to match model outcomes with available empirical evidence – offers considerable potential
379 for making predictions regarding the population dynamics for other emerging diseases,
380 including those with more rapid eco-epidemiological dynamics (Toni et al. 2009, Beaumont
381 2010, Johnson and Briggs 2011, Wells et al. 2015). A fundamental problem in applying
382 modelling approaches to forecast the outcome of emerging infectious disease epidemics is the
383 need to estimate parameter values based on empirical data derived from the relatively early
384 stages of an epizootic, in the absence of retrospective knowledge (Heesterbeek et al. 2015,
385 Ferguson et al. 2016). Examples include estimating R_0 for SARS (Lipsitch et al. 2003) and
386 for the 2014-2015 Ebola epidemic in West Africa (Whitty et al. 2014, WHO Ebola Response
387 Team 2014) among others (LaDeau et al. 2011). In most of these cases, the objective is to
388 estimate parameters associated with the growth phase of the epidemic to assess the
389 effectiveness of interventions such as vaccination. The task we have addressed in this paper is
390 even more challenging – seeking to predict the long-term endemic behaviour of a pathogen
391 that is currently still in the early stages of emergence. We suggest that management efforts to
392 maintain devil populations in the face of DFTD should be guided by our changing
393 understanding of the long-term dynamics of the DFTD epidemic. Management efforts in wild
394 populations that solely aim to combat the impact of DFTD can be counterproductive if they
395 disrupt long-term eco-evolutionary dynamics that may eventually lead to endemicity with
396 stable devil populations. Our ability to predict future outcomes in the absence of management
397 actions require some caution as we cannot fully exclude the possibility that DFTD can cause
398 local population extinctions once populations are small, warranting future research. While
399 our findings emphasize the importance of accounting for individual tumour load for accurate

prediction and epidemiological modelling of DFTD dynamics, our inability to uncover the exact role of devil spatial proximity on disease transmission means that further research is necessary to understand relevant factors in disease spread.

The key management implication of our model is that "heroic" management interventions are unlikely to be necessary to ensure persistence of Tasmanian devil populations with regard to DFTD control. Given more information on immune-related or genetic variation in resistance, the model could be modified to assess the value of interventions such as vaccination or reintroduction of captive reared animals. At the same time, we believe that any management actions should be subject to rigorous quantitative analysis to explore possible long-term impacts. In particular, allocating resources and scientific endeavours to the management of wildlife diseases such as DFTD should not disguise the fact that sufficiently large and undisturbed natural environments are a vital prerequisite for wildlife to persist and eventually cope with perturbations such as infectious diseases without human intervention.

ACKNOWLEDGMENTS

The study was funded by NSF grant DEB 1316549 and NIH grant R01 GM126563-01 as part of the joint NIH-NSF-USDA Ecology and Evolution of Infectious Diseases Program, NIH grant P30GM103324, the Australian Research Council Discovery (DP110102656), Future Fellowship (FT100100250), DECRA (DE17010116) and Linkage (LP0561120, LP0989613) Schemes, the Fulbright Scholarship Scheme, the Ian Potter Foundation, the Australian Academy of Science (Margaret Middleton Fund), two grants from the Estate of W.V. Scott, the National Geographic Society, the Mohammed bin Zayed Conservation Fund, the Holsworth Wildlife Trust and three Eric Guiler Tasmanian Devil Research Grants through the

Save the Tasmanian Devil Appeal of the University of Tasmania Foundation. We are grateful for all support during field work underpinning this modelling study: M. and C. Walsh, Discovery Holidays Parks-Cradle Mountain National Park, and Forico Pty Ltd provided logistic support and many volunteers helped with data collection (published previously). Comments from Samuel Alizon and anonymous reviewers improved previous drafts.
K.W. conceived the idea of this study, carried out the analysis and wrote the first draft. All authors interpreted results and contributed to revisions. All authors gave final approval for publication.

DATA ACCESSIBILITY

Data and R code supporting the results are available as supporting material Data S1 (table of summary statistics derived from empirical field study) and Data S2 (R Code for running simulation and analysing the simulation outcomes).

LITERATURE CITED

449 Anderson, R. M., and R. M. May. 1978. Regulation and stability of host-parasite population
450 interactions: 1. regulatory processes. Journal of Animal Ecology 47:219-247.
451 Anderson, R. M., and R. M. May. 1991. Infectious diseases of humans: dynamics and
452 control. Oxford University Press, Oxford.
453 Bailey, N. T. J. 1975. The mathematical theory of infectious diseases and its applications. 2nd
454 edition. Charles Griffin.
455 Beaumont, M. A. 2010. Approximate Bayesian Computation in evolution and ecology.
456 Annual Review of Ecology, Evolution, and Systematics 41:379-406.
457 Beeton, N., and H. McCallum. 2011. Models predict that culling is not a feasible strategy to
458 prevent extinction of Tasmanian devils from facial tumour disease. Journal of Applied
459 Ecology 48:1315-1323.
460 Benton, T. G., S. J. Plaistow, and T. N. Coulson. 2006. Complex population dynamics and
461 complex causation: devils, details and demography. Proceedings of the Royal Society
462 Biological Sciences Series B. 273:1173-1181.
463 Briggs, C. J., R. A. Knapp, and V. T. Vredenburg. 2010. Enzootic and epizootic dynamics of
464 the chytrid fungal pathogen of amphibians. Proceedings of the National Academy of
465 Sciences 107:9695-9700.
466 Campbell-Staton, S. C., Z. A. Cheviron, N. Rochette, J. Catchen, J. B. Losos, and S. V.
467 Edwards. 2017. Winter storms drive rapid phenotypic, regulatory, and genomic shifts
468 in the green anole lizard. Science 357:495-498.
469 Cazelles, B., and S. Hales. 2006. Infectious diseases, climate influences, and nonstationarity.
470 Plos Medicine 3:e328.
471 Christie, M. R., M. L. Marine, S. E. Fox, R. A. French, and M. S. Blouin. 2016. A single
472 generation of domestication heritably alters the expression of hundreds of genes.
473 Nature Communications 7:10676.

474 Csillery, K., O. Francois, and M. G. B. Blum. 2012. abc: an R package for approximate
475 Bayesian computation (ABC). Methods in Ecology and Evolution 3:475-479.
476 de Castro, F., and B. Bolker. 2005. Mechanisms of disease-induced extinction. Ecology
477 Letters 8:117-126.
478 Drawert, B., M. Griesemer, L. R. Petzold, and C. J. Briggs. 2017. Using stochastic
479 epidemiological models to evaluate conservation strategies for endangered
480 amphibians. Journal of the Royal Society Interface 14.
481 Elith, J., J. R. Leathwick, and T. Hastie. 2008. A working guide to boosted regression trees.
482 Journal of Animal Ecology 77:802-813.
483 Epstein, B., M. Jones, R. Hamede, S. Hendricks, H. McCallum, E. P. Murchison, B.
484 Schönfeld, C. Wiench, P. Hohenlohe, and A. Storfer. 2016. Rapid evolutionary
485 response to a transmissible cancer in Tasmanian devils. Nature Communications
486 7:12684.
487 Fenner, F. 1983. Biological control as exemplified by smallpox eradication and myxomatosis.
488 Proceedings of the Royal Society B: Biological Sciences 218:259-285.
489 Ferguson, N. M., Z. M. Cucunubá, I. Dorigatti, G. L. Nedjati-Gilani, C. A. Donnelly, M.-G.
490 Basáñez, P. Nouvellet, and J. Lessler. 2016. Countering the Zika epidemic in Latin
491 America. Science 353:353-354.
492 Gandon, S., M. E. Hochberg, R. D. Holt, and T. Day. 2013. What limits the evolutionary
493 emergence of pathogens? Philosophical Transactions of the Royal Society B:
494 Biological Sciences 368.
495 Gilchrist, M. A., and D. Coombs. 2006. Evolution of virulence: interdependence, constraints,
496 and selection using nested models. Theoretical Population Biology 69:145-153.

497 Gog, J. R., L. Pellis, J. L. N. Wood, A. R. McLean, N. Arinaminpathy, and J. O. Lloyd-
498 Smith. 2015. Seven challenges in modeling pathogen dynamics within-host and across
499 scales. Epidemics 10:45-48.
500 Grimm, V., U. Berger, F. Bastiansen, S. Eliassen, V. Ginot, J. Giske, J. Goss-Custard, T.
501 Grand, S. K. Heinz, G. Huse, A. Huth, J. U. Jepsen, C. Jorgensen, W. M. Mooij, B.
502 Mueller, G. Pe'er, C. Piou, S. F. Railsback, A. M. Robbins, M. M. Robbins, E.
503 Rossmanith, N. Rueger, E. Strand, S. Souissi, R. A. Stillman, R. Vabo, U. Visser, and
504 D. L. DeAngelis. 2006. A standard protocol for describing individual-based and
505 agent-based models. Ecological Modelling 198:115-126.
506 Hamede, R., J. Bashford, M. Jones, and H. McCallum. 2012. Simulating devil facial tumour
507 disease outbreaks across empirically derived contact networks. Journal of Applied
508 Ecology 49:447-456.
509 Hamede, R. K., N. J. Beeton, S. Carver, and M. E. Jones. 2017. Untangling the model
510 muddle: empirical tumour growth in Tasmanian devil facial tumour disease. Scientific
511 Reports 7:6217.
512 Hamede, R. K., H. McCallum, and M. Jones. 2013. Biting injuries and transmission of
513 Tasmanian devil facial tumour disease. Journal of Animal Ecology 82:182-190.
514 Hamede, R. K., A.-M. Pearse, K. Swift, L. A. Barmuta, E. P. Murchison, and M. E. Jones.
515 2015. Transmissible cancer in Tasmanian devils: localized lineage replacement and
516 host population response. Proceedings of the Royal Society of London B: Biological
517 Sciences 282:20151468.
518 Hastings, A. 2004. Transients: the key to long-term ecological understanding? Trends in
519 Ecology & Evolution 19:39-45.
520 Hawkins, C. E., C. Baars, H. Hesterman, G. J. Hocking, M. E. Jones, B. Lazenby, D. Mann,
521 N. Mooney, D. Pemberton, S. Pyecroft, M. Restani, and J. Wiersma. 2006. Emerging

522 disease and population decline of an island endemic, the Tasmanian devil *Sarcophilus*
523 *harrisii*. Biological Conservation 131:307-324.
524 Heesterbeek, H., R. M. Anderson, V. Andreasen, S. Bansal, D. De Angelis, C. Dye, K. T. D.
525 Eames, W. J. Edmunds, S. D. W. Frost, S. Funk, T. D. Hollingsworth, T. House, V.
526 Isham, P. Klepac, J. Lessler, J. O. Lloyd-Smith, C. J. E. Metcalf, D. Mollison, L.
527 Pellis, J. R. C. Pulliam, M. G. Roberts, C. Viboud, and I. N. I. I. Collaboration. 2015.
528 Modeling infectious disease dynamics in the complex landscape of global health.
529 Science 347.
530 Heesterbeek, J. A. P. 2002. A brief history of R0 and a recipe for its calculation. Acta
531 Biotheoretica 50:189-204.
532 Johnson, L. R., and C. J. Briggs. 2011. Parameter inference for an individual based model of
533 chytridiomycosis in frogs. Journal of Theoretical Biology 277:90-98.
534 Jones, M. E., A. Cockburn, R. Hamede, C. Hawkins, H. Hesterman, S. Lachish, D. Mann, H.
535 McCallum, and D. Pemberton. 2008. Life-history change in disease-ravaged
536 Tasmanian devil populations. Proceedings of the National Academy of Sciences of
537 the United States of America 105:10023-10027.
538 Kerr, P. J. 2012. Myxomatosis in Australia and Europe: a model for emerging infectious
539 diseases. Antiviral Research 93:387-415.
540 LaDeau, S. L., G. E. Glass, N. T. Hobbs, A. Latimer, and R. S. Ostfeld. 2011. Data-model
541 fusion to better understand emerging pathogens and improve infectious disease
542 forecasting. Ecological Applications 21:1443-1460.
543 Langwig, K. E., W. F. Frick, R. Reynolds, K. L. Parise, K. P. Drees, J. R. Hoyt, T. L. Cheng,
544 T. H. Kunz, J. T. Foster, and A. M. Kilpatrick. 2015. Host and pathogen ecology drive
545 the seasonal dynamics of a fungal disease, white-nose syndrome. Proceedings of the
546 Royal Society B-Biological Sciences 282.

547 Lazenby, B. T., M. W. Tobler, W. E. Brown, C. E. Hawkins, G. J. Hocking, F. Hume, S.
548 Huxtable, P. Iles, M. E. Jones, C. Lawrence, S. Thalmann, P. Wise, H. Williams, S.
549 Fox, and D. Pemberton. 2018. Density trends and demographic signals uncover the
550 long-term impact of transmissible cancer in Tasmanian devils. Journal of Applied
551 Ecology:n/a-n/a.
552 Lipsitch, M., T. Cohen, B. Cooper, J. M. Robins, S. Ma, L. James, G. Gopalakrishna, S. K.
553 Chew, C. C. Tan, M. H. Samore, D. Fisman, and M. Murray. 2003. Transmission
554 dynamics and control of severe acute respiratory syndrome. Science 300:1966-1970.
555 Lloyd-Smith, J. O., P. C. Cross, C. J. Briggs, M. Daugherty, W. M. Getz, J. Latto, M. S.
556 Sanchez, A. B. Smith, and A. Swei. 2005. Should we expect population thresholds for
557 wildlife disease? Trends in Ecology & Evolution 20:511-519.
558 McCallum, H., and B. A. Hocking. 2005. Reflecting on ethical and legal issues in wildlife
559 disease. Bioethics 19:336-347.
560 McCallum, H., and M. Jones. 2006. To lose both would look like carelessness: Tasmanian
561 devil facial tumour disease. Plos Biology 4:1671-1674.
562 McCallum, H., M. Jones, C. Hawkins, R. Hamede, S. Lachish, D. L. Sinn, N. Beeton, and B.
563 Lazenby. 2009. Transmission dynamics of Tasmanian devil facial tumor disease may
564 lead to disease-induced extinction. Ecology 90:3379-3392.
565 Mideo, N., S. Alizon, and T. Day. 2008. Linking within- and between-host dynamics in the
566 evolutionary epidemiology of infectious diseases. Trends in Ecology & Evolution
567 23:511-517.
568 Murdoch, W. W., C. J. Briggs, and R. M. Nisbet. 2003. Consumer-resource dynamics.
569 Princeton University Press.
570 Pearse, A. M., and K. Swift. 2006. Allograft theory: transmission of devil facial-tumour
571 disease. Nature 439:549-549.

572 Pye, R., R. Hamede, H. V. Siddle, A. Caldwell, G. W. Knowles, K. Swift, A. Kreiss, M. E.
573 Jones, A. B. Lyons, and G. M. Woods. 2016. Demonstration of immune responses
574 against devil facial tumour disease in wild Tasmanian devils. Biology letters 12.
575 R Development Core Team. 2017. R: A language and environment for statistical computing.
576 R Foundation for Statistical Computing, Vienna, Austria.
577 Roesch, A., and H. Schmidbauer. 2014. WaveletComp: computational wavelet analysis. R
578 package version 1.0.
579 Smith, K. F., K. Acevedo-Whitehouse, and A. B. Pedersen. 2009. The role of infectious
580 diseases in biological conservation. Animal Conservation 12:1-12.
581 Toni, T., D. Welch, N. Strelkowa, A. Ipsen, and M. P. H. Stumpf. 2009. Approximate
582 Bayesian computation scheme for parameter inference and model selection in
583 dynamical systems. Journal of the Royal Society Interface 6:187-202.
584 Wells, K., B. W. Brook, R. C. Lacy, G. J. Mutze, D. E. Peacock, R. G. Sinclair, N.
585 Schwensow, P. Cassey, R. B. O'Hara, and D. A. Fordham. 2015. Timing and severity
586 of immunizing diseases in rabbits is controlled by seasonal matching of host and
587 pathogen dynamics. Journal of the Royal Society Interface 12:20141184.
588 Wells, K., R. Hamede, D. H. Kerlin, A. Storfer, P. A. Hohenlohe, M. E. Jones, and H. I.
589 McCallum. 2017. Infection of the fittest: devil facial tumour disease has greatest
590 effect on individuals with highest reproductive output. Ecology Letters 20:770–778.
591 Whitty, C. J. M., J. Farrar, N. Ferguson, W. J. Edmunds, P. Piot, M. Leach, and S. C. Davies.
592 2014. Tough choices to reduce Ebola transmission. Nature 515:192–194.
593 WHO Ebola Response Team. 2014. Ebola virus disease in West Africa - the first 9 months of
594 the epidemic and forward projections. New England Journal of Medicine 371:1481-
595 1495.

Wilber, M. Q., K. E. Langwig, A. M. Kilpatrick, H. I. McCallum, and C. J. Briggs. 2016. Integral projection models for host-parasite systems with an application to amphibian chytrid fungus. Methods in Ecology and Evolution 10:1182–1194

Wood, S. N. 2010. Statistical inference for noisy nonlinear ecological dynamic systems. Nature 466:1102–1104.

Wright, B., C. E. Willet, R. Hamede, M. Jones, K. Belov, and C. M. Wade. 2017. Variants in the host genome may inhibit tumour growth in devil facial tumours: evidence from genome-wide association. Scientific Reports 7:423.

FIGURE CAPTION

Figure 1. Illustrative overview of the individual-based model to explore long-term population changes of a Tasmanian devil population burdened with devil facial tumour disease (DFTD). Individuals are distributed in a study area. For every weekly time step seven different processes are modelled, namely 1) the possible recruitment of young from females (conditional on young survival during previous weaning time), 2) possible death independent of disease status, 3) movement of individuals away from their home range centre, 4) behavioural interaction between nearby individuals that may result in the transmission of DFTD, 5) growth of DFTD tumours, 6) death of individuals resulting from DFTD, 7) aging of individuals.

Figure 2. Frequency distributions of timespans of devil extirpation (upper panel) and devil facial tumour disease (DFTD) extirpation (lower panel) presented as years after the introduction of the disease into populations. Number of plotted scenarios correspond to those for which extirpation events were recorded (26 and 69 out of 122 posterior samples, respectively).

Figure 3. Examples of long-term devil and tumour dynamics. Scenario 1 is an example of DFTD extirpation, and Scenario 2 is an example of coexistence. The upper panels show the summarized population sizes (free-ranging individuals $\geq$ 35 weeks old) over 100 years (5,200 weeks) of simulations after the introduction of DFTD in the population, middle panels show the respective wavelet power spectra, based on Morlet wavelet analysis. Red spectral colours in the power spectra indicate strong periodicity over weekly time spans depicted on the y-axis and the corresponding time during the course of simulations indicated on the x-axis; blue spectral colours indicate weak periodicity. Ridges (black lines) of strongest periodicity often

646 indicate long-term oscillations > 500 weeks. Lower panels show the prevalence of DFTD
647 (growing tumour ≥ 0.1 cm^3) in the respective population.
648
649 **Figure 4.** Frequency distributions (count) of mean devil populations sizes (x axis, upper
650 panel) and mean devil facial tumour disease (DFTD) prevalence (x axis, lower panel) 80-100
651 years after disease introduction for those scenarios (n = 27) in which DFDT persisted for at
652 least 100 years. The light-grey vertical line in the upper panel indicates the mean population
653 sizes of simulated populations over 100 years prior to disease introduction.
654
655
656
657
658
659
660
661
662
663
664

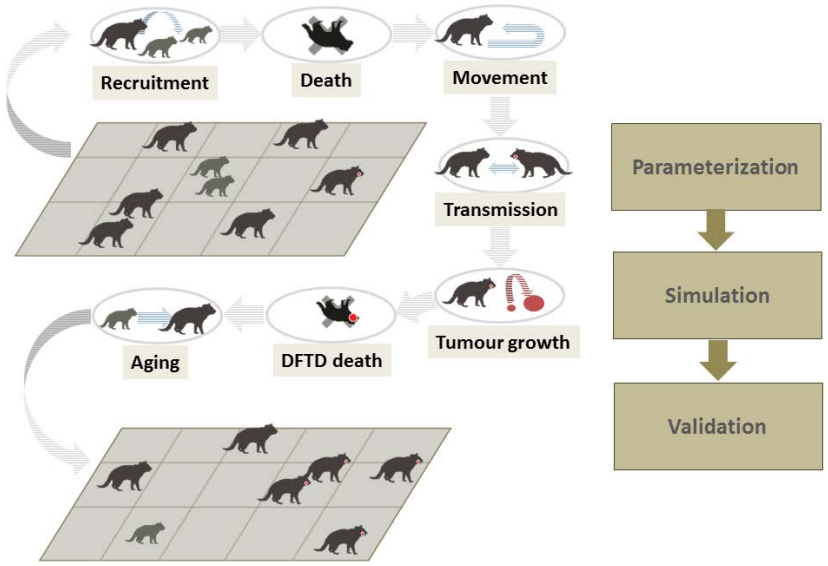

665

666 **Figure 1.**

667

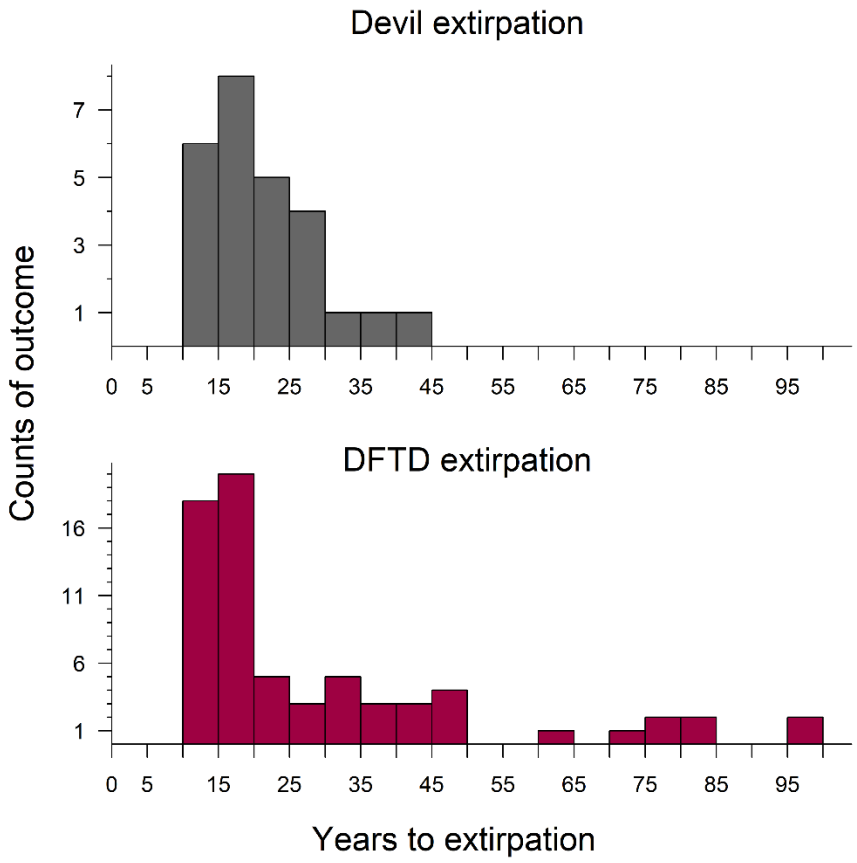

668

669 **Figure 2.**

670

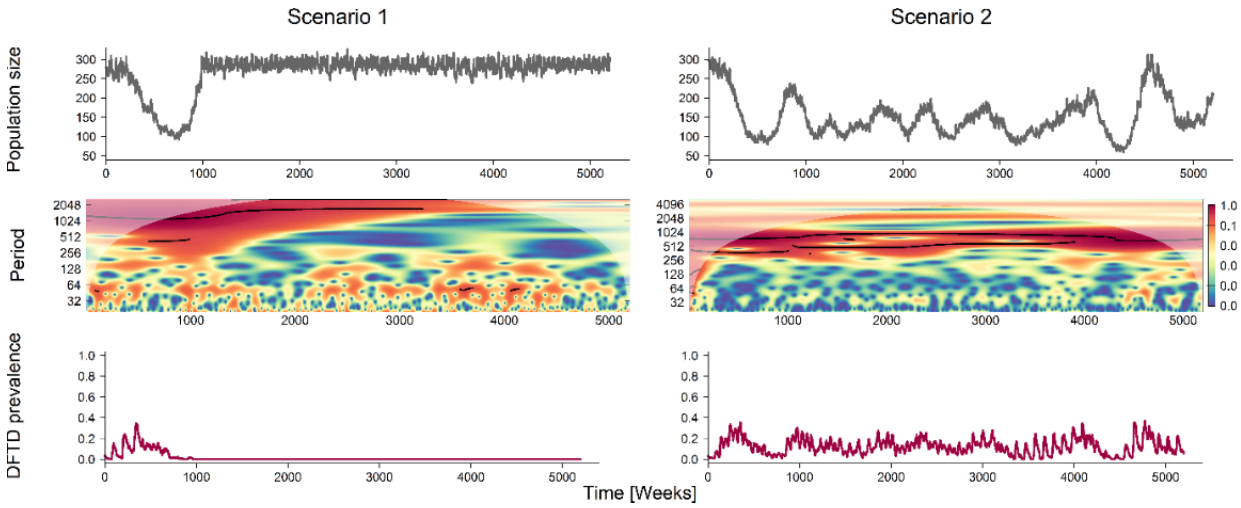

671

672 **Figure 3.**

673

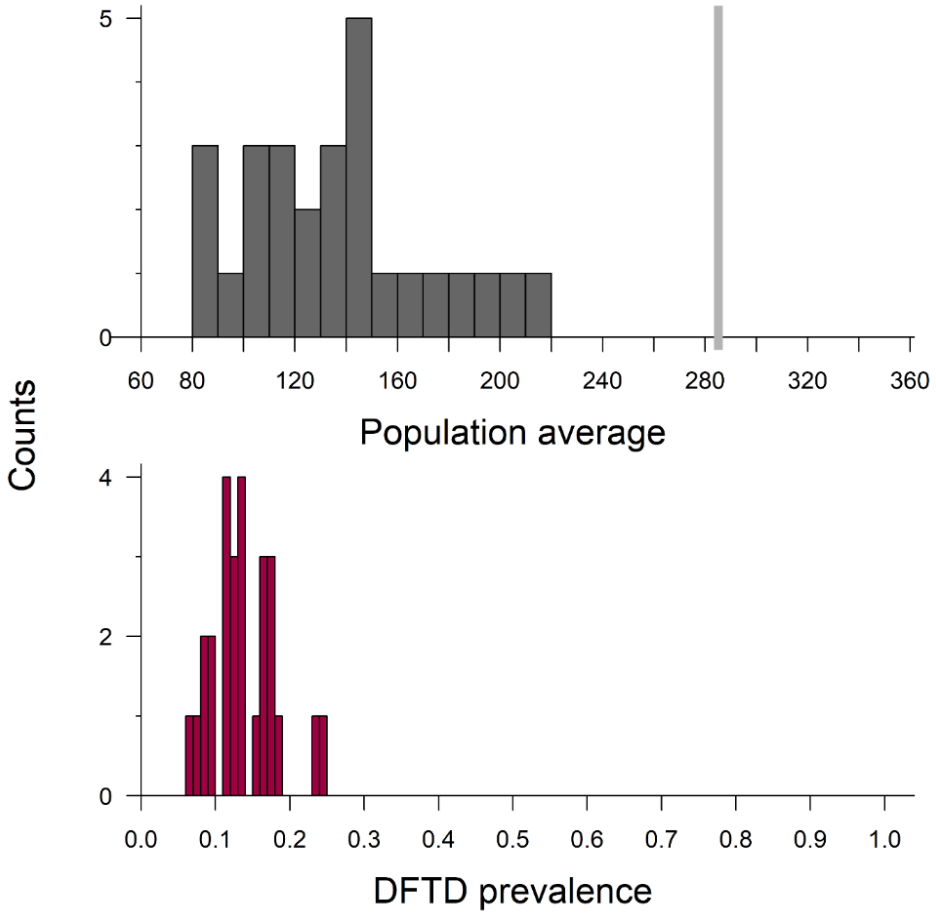

674

675 **Figure 4.**